Three Coils, High-Resolution Receiver Positioning System for Wireless Power Transfer

Jiaxing Zhang, Jiayang Li, Dai Jiang, and Andreas Demosthenous

Department of Electronic and Electrical Engineering, University College London, Torrington Place, London WC1E 7JE, UK

e-mail: jiaxing.zhang.22@ucl.ac.uk; a.demosthenous@ucl.ac.uk

***Abstract*—Wireless power transfer with inductively coupled coils is widely used for powering implantable devices. For a continuously moving receiver coil (Rx), real-time detection of its position is important for the magnetic field distribution control. This paper proposes an Rx positioning system that uses three varying-pitch coils and applies a trilateration algorithm for positioning. It operates at a frequency of 125 kHz. The detection area is approximately 224 cm^2, when using a 2 cm radius Rx. Experimental results show the position detection system has a 1 cm^2 resolution with an average deviation of 6.8 mm.**

Keywords—Inductive coupling, maximum power point tracking (MPPT), moving Rx tracking algorithm, overlapping Tx array.

I. Introduction

Neural and brain interfaces serve as a channel to capture analogue signals from the brain and communicate with electronic devices. Novel brain-computer interfaces have the potential to diagnose and treat neurological disorders. Typically, experiments involving neural interfaces are conducted on rodents. Cables constrain the movements of an animal, and battery-powered implants have limited operating time, bulky size, and complication risks. Wireless power transfer is a preferred solution for animal experiments with implantable devices.

Inductive coupling power transfer (ICPT) has been widely used in animal experiments. Power transfer efficiency (PTE) is greatly affected by the coupling coefficient (k) between the transmitter coil (Tx) and receiver coil (Rx) [1]. When the Rx is implanted in an animal, k fluctuates with animal movement. To increase the magnetic flux density and k near the Rx, the Rx position is critical information.

In [2], a Tx array of overlapping planar coils with magnetic sensors was proposed. The system tracks the position of the receiver through an array of 27 magnetic sensors, which results in a bulky system. Another design in [3] has five Tx and four Rx with varying heights and orientations to ensure a constant k when Rx is moving and rotating. The limitation of this system is that it cannot provide the position. In [4], a four-layer 15 Txs array with a tracking algorithm was proposed to track the position of Rx. The system scans nine Txs each time to activate the Tx with the highest k. However, the resolution of tracking is the same as the size of Tx. Alternatively, using cameras to detect the position of the animal, introduces additional costs for devices and installation [5].

This paper proposes a novel Rx tracking system as shown in Fig. 1. The system achieves Rx positioning with only three detection Txs, offering a low cost, lightweight design. Each Tx system incorporates a varying-pitch spiral Tx design to enhance the coil coupling at its edge. A trilateration algorithm calculates the Rx position.

The rest of this paper is organized as follows. Section II presents the theory of the resonant circuit, the varying-pitch coil and the positioning algorithm. Section III describes the circuit for lateral misalignment measurement. Section IV discusses the experimental results. Section V summarises the paper with concluding remarks.

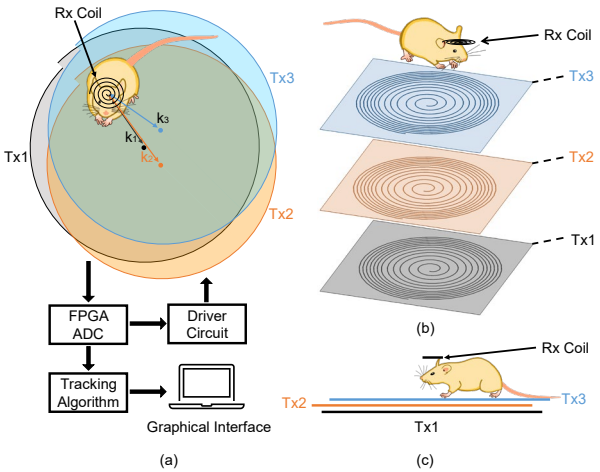

Fig. 1. (a) Top view of Tx array and functional diagram of the positioning system. The illustration shows the centre and outline of Tx coils to highlight the proposed configuration. (b) 3-D view. (c) Front view.

II. Theory

A. Resonant Circuit Configuration

ICPT is based on a pair of inductively-coupled Tx-Rx working at their resonant frequency. The proposed system contains three Tx modules and a Rx module. Fig. 2(a) shows the inductive link between Tx1 and Rx as an example. The mutual inductance between Txs is not included, because other Txs are in open circuit when Tx1 is working. Both Tx1 and Rx are composed of a coil (L_1 and L_{Rx}) with its resistance (R_1 and R_{Rx}) and tuning capacitors (C_{11}, C_{12} and C_{Rx}). Z_L represents the load impedance, Z_{in} is the input impedance of the inductive link. The current I is supplied by a class-D power amplifier. The voltage on tuning capacitor C_{12} is:

$$|V_{C12}| = |I|X_{C12} = X_{C12}\frac{|V_{in}|}{Z_{in}} = X_{C12}\frac{|V_{in}|}{R_1 + R_{refl}} \quad (1)$$

where X_{C12} is the reactance of C_{12}, and

$$R_{refl} = \frac{(\omega M)^2}{R_{Rx} + Z_L}. \quad (2)$$

M is the mutual inductance between the Tx and the Rx. $|I|$, $|V_{C12}|$, and $|V_{in}|$ represent the peak current amplitude on Tx, the peak voltages on C_{12} and the class-D power amplifier supply voltage respectively. From (1) and (2), M can be obtained as:

$$M = k\sqrt{L_1 L_{Rx}} = \sqrt{\frac{\left(\frac{|V_{in}|X_{C12}}{|V_{C12}|} - R_1\right)(R_{Rx}+Z_L)}{\omega^2}}. \quad (3)$$

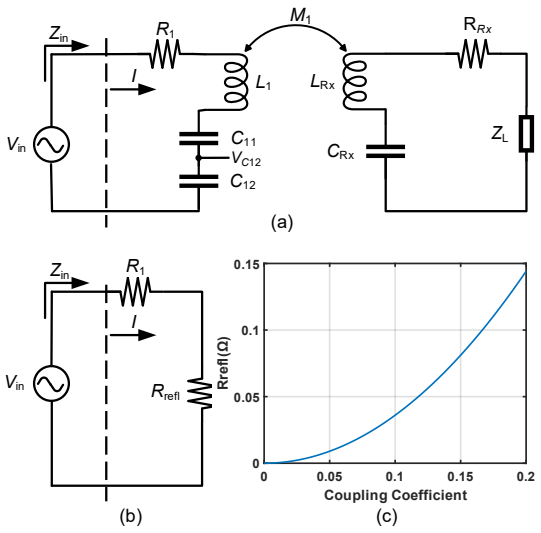

Fig. 2. (a) Resonant circuit of Tx1 and Rx. (b) Equivalent circuit of inductive link of Tx1 with Rx. (c) Simulation of Rrefl variation on Tx (conventional spiral coil) side.

TABLE I. COIL AND SYSTEM SPECIFICATIONS

Operating frequency	125 kHz
Angular frequency (ω)	785398 rad/s
Tx radius (a)	105 mm
Rx radius (b)	20 mm
Tx inductance (L_1)	15.49 µH
Rx inductance (L_{Rx})	3.5 µH
Tx input voltage ($\lvert V_{in} \rvert$)	0.22 V
Tx1 resistance (R_1)	0.590 mΩ
Rx resistance (R_{RX})	0.300 mΩ
Load impedance (Z_L)	10 Ω
System power	0.434 W
Positioning area	224 cm^2

The parameters used in (3) are listed in Table. I. M and k can be derived by measuring the V_{C12} on the Tx. From [6] the relationship of lateral misalignment between two coils can be expressed as:

$$d = \frac{(\mu_0 abG(\gamma))^2}{M^2 a} - b \tag{4}$$

where

$$G(\gamma) = \left(\frac{2}{\gamma} - \gamma\right) K(\gamma) - \frac{2}{\gamma} E(\gamma) \tag{5}$$

$$\gamma = \sqrt{\frac{4a(b+d)}{(a+b+d)^2 + h^2}}. \tag{6}$$

μ_0 is the free-space permeability, a and b are radius of two coils, h and d are the vertical distance and lateral misalignment between two coils, and $K(\gamma)$ and $E(\gamma)$ are complete elliptic integrals of the first and second kind, respectively. From (3) and (4), the lateral misalignment can be calculated by measuring V_{C12}.

In conventional spiral coil windings k changes from 0 to 0.2 when the centre of the Rx moves from the edge to the centre of the Tx. The variation of R_{refl} with changing k is shown in Fig. 2(c). When k is in the region of 0-0.05, R_{refl} is within 0-0.02 Ω. Over this range, the voltage change is challenging to observe. Therefore, the k variation at the edge must be improved for better observation.

B. Coil Design

M at the edge can be increased by increasing the total number of turns for Tx. However, more turns result in a higher resistance and reduce the variation of k at the centre of Tx, making it challenging to calculate d. The total mutual inductance M_T between Tx and Rx is:

$$M_T = \sum_{m=1}^{N_{TX}} \sum_{n=1}^{N_{Rx}} M(a_m, b_n, h, d) \tag{7}$$

where N_{TX} and N_{Rx} are total turns of the Tx and Rx, a_m and b_n are the radius of the coil for m and n turns.

From (7), the mutual inductance can be increased by increasing the number of turns. In addition, from [6], the mutual inductance is higher when d is small. Hence, it is possible to enhance k by increasing the density of turns at the edge of Tx.

To ensure a high Q factor the optimal turn of Tx coils is around 12 (from analysis in [1]) when the wire diameter is 0.5 mm, which is used to make the coil in this study. From Fig. 3(a) k drops by half when d equals 50 mm, and k is below 0.05 when d equals 80 mm, which only has a R_{refl} of 0.02 Ω. Hence, k needs to be improved at these two points. A novel varying-pitch spiral is proposed as shown in Fig. 3(c) and (d) based on

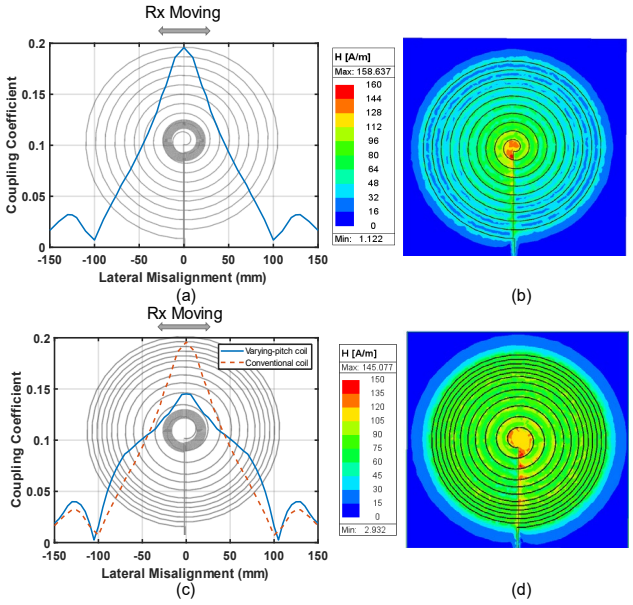

Fig. 3. Simulated k dependence of lateral misalignment and the magnetic field (H). h between Tx and Rx is 3 mm. (a) and (b) Conventional spiral coil. (c) and (d) Proposed spiral coil.

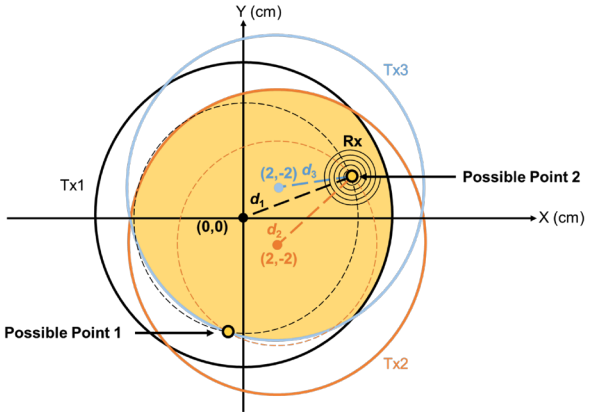

Fig. 4. Trilateration positioning algorithm. Tx coils are represented by a circle outline with their centre. Dashed lines represent the lateral misalignment measured by positioning system. The intersection of three Txs which is shown in yellow represents the available positioning area.

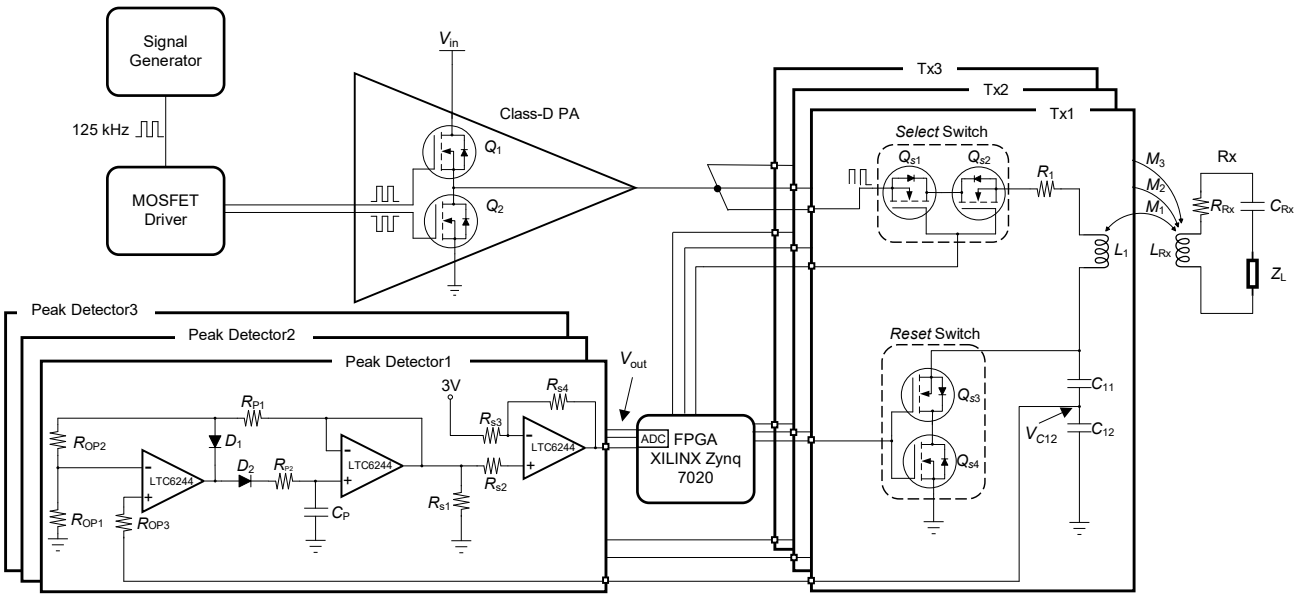

Fig. 5. The proposed positioning system schematic consists of a Tx driver, peak detectors, switches, Rx, and a FPGA for control.

the analysis above. The radius of the varying-pitch coil starts from 1 cm, the pitch for the inner 3 turns is 15 mm, for the middle 3 turns it is 10 mm, and for the outer 4 turns is 6 mm. The magnetic field generated by this varying-pitch coil is simulated and compared with the field from a constant-pitch coil using Ansys Maxwell software, as shown in Fig. 3(b) and (d). The magnetic flux density is notably enhanced at the edge of Tx, and k decreases at the centre, which meets the requirements mentioned before. In Fig. 3(c), the simulation results compare the k between Tx and Rx with two different coils. When Rx is located at a lateral misalignment of 80 mm with a h of 3 mm, k improves from 0.04 to 0.07.

C. Rx Positioning Algorithm

At least three distance data are needed for positioning a point in a space. Hence, the system employs three displaced Txs for positioning. Fig. 4 shows their position. In the following analysis, h between Tx and Rx is assumed to be fixed for simplicity. From (4), k is influenced solely by d. The positioning system records the output voltage V_{out} of each Tx when there is no Rx, and when Rx is at the centre of each; these two voltages are the maximum and minimum values of each Tx. The system assumes the voltage change is linear when Rx moves from the centre to the edge. The lateral misalignment is mapped to the voltage in this way.

The system acquires the lateral misalignment of each Tx with Rx, d_1, d_2, and d_3. With the centre information of the Txs in Fig. 4, the first Tx establishes a possible location circle of Rx. The second Tx narrows down the possible circle to the intersection points of two circles. The third Tx compares d_3 with the distance from the centre of Tx3 to two possible points and chooses the point with minimum deviation as the Rx coordinate.

Each Tx is activated in turn to measure d with Rx. A control signal ensures only one Tx is active at any time to maintain zero mutual inductance between Txs. The active time of each Tx is set to 0.01 s. The system continuously acquires the Rx location with a frequency of 33 Hz. The positioning area is restricted to the intersection of three Txs as shown in Fig. 4 because k is near zero when Rx is located outside a Tx. For a continuously moving object, the system records the direction of movement. Therefore, the system has the potential to scale up to a large positioning area by predicting the next active area.

III. Detection System Design

The circuit of the proposed system is shown in Fig. 5. It consists of a class-D power amplifier, 3 Tx modules and their associated peak detectors, a Rx, and a FPGA (XILINX Zynq 7020) to implement the tracking algorithm. The detection circuit consists of a dual inverting MOSFET driver (MAX17602), two NMOS power transistors (BSC117) serving as the class-D power amplifier, an analogue multiplexer (MAX4617) and four power transistors (SIR164) utilized as a channel selector.

A. Tx Selection Circuit

There are two pairs of power transistors (Q_{s1}, Q_{s2}), (Q_{s3}, Q_{s4}) in each Tx module for a *Select* switch and a *Reset* switch as shown in Fig. 5. In each switch, two power transistors are connected in series at the drains to prevent the coupling current passing through the body diode at the off state and avoid crosstalk between various Tx. The *Select* switch activates the Tx module, and the *Reset* switch discharges the tuning capacitors when the Tx module is inactive to ensure the circuit turns on in the same initial state. The gates of the transistors are controlled by the FPGA.

B. Tx Voltage Sensing

The tuning capacitors C_{11} and C_{12} are set at 110 nF and 2.2 μF respectively for a total capacitance of 104.8 nF, ensuring Tx operates at its resonant frequency. C_{11} and C_{12} form a potential divider to the input voltage of the peak detector, ensuring V_{C12} is within the supply range of the operational amplifiers. Using a current sensing resistor, would introduce attenuation in the Tx circuit [8], additional power cost and reduce voltage variation when Rx changes. Sensing the voltage across the tuning capacitor avoids these problems. The peak detectors consist of three op-amps (LTC6244). The first op-amp has a gain of 20 for high detection accuracy. The second op-amp is a peak detector which captures and holds the peak of V_{C12}. The third op-amp subtracts 3 V from the output of the peak detector to adjust it to the input range of the FPGA ADC of 0-1 V.

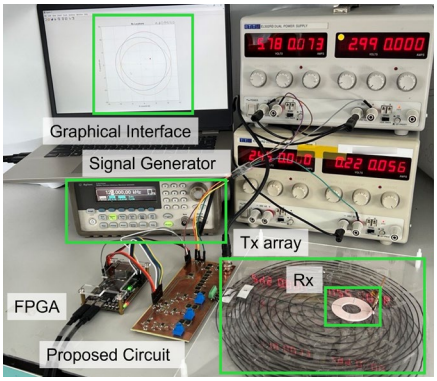

Fig. 6. Experimental setup.

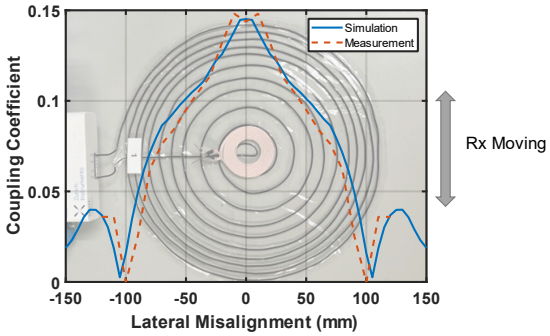

Fig. 7. k comparison between measurement and simulation.

IV. Experimental Results

The experimental setup to validate the coil performance and positioning system, is shown in Fig. 6. Txs are fixed to the base, and centre positions of three Txs are the same as detailed in Fig. 5. An acrylic plate, 2 mm thick, is placed above the Tx array using a 10 mm pillar to represent the gap between the implanted Rx coil and Txs. An impedance analyser (Zurich Instruments MFIA) was used to measure the mutual inductance between Tx and Rx to calculate k as shown in Fig. 7. The measurements compared well with the simulations. The coupling coefficient is 0.065 when lateral misalignment is 80 mm, which meets the requirement of improving k at the edge of Tx.

The system records the V_{out} when Rx moves, mapping the voltage with the lateral misalignment. The positioning system was tested by moving the Rx from the centre of Tx to the edge and the output voltage was recorded in 5 mm steps. As shown in Fig. 8(a), the recorded output voltage of Tx1 increases approximately linearly at 10 mV per 5 mm step when lateral misalignment changes from 1 to 9 cm, suggesting a detection resolution at the mm level of one Tx.

To test the minimum resolution of the system, test points were set every 1 cm on the x-axis and 2 cm on the y-axis. Detected positions of the Rx given by the system at these points were compared with the actual positions, and then the deviation was calculated and plotted in Fig. 8(b), where the colour indicates the level of deviation. The deviation of the test points is used to approximate the average deviation in the area between these points. There are some areas which have a higher deviation because the shape of the coils does not perfectly correspond to the design shape, which causes an uneven magnetic field. The connecting wires under the coils cause a magnetic field change at the middle-left part of the coil, and higher deviations in this area. The overall average deviation of the positioning area is 6.8 mm.

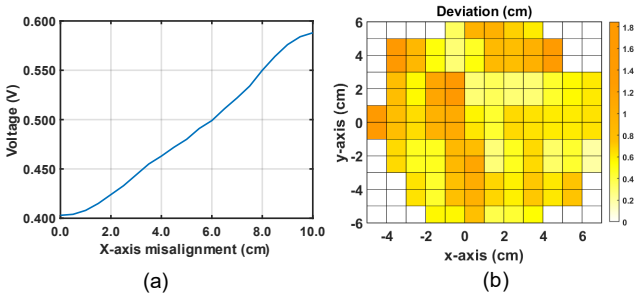

Fig. 8. (a) V_{out} respect to d. (b) System average deviation.

TABLE II. Performance Summary and Comparison

Reference	2016 [7]	2018 [9]	2022 [4]	This work
Positioning method	Reflected impedance	Magnetic Sensors	Reflected impedance	Reflected impedance
Number of Tx	16	12[a]	15	3
Positioning area (cm^2)	756	127	600	224
Resolution (cm^2)	47.25	15	40	1

[a] Number of Magnetic Sensors

V. Conclusion

In this paper, a lightweight Rx position detection system is proposed using three displaced Txs. A novel varying-pitch Tx is designed to improve the accuracy of the system. A trilateration positioning algorithm is applied to determine the Rx position. The system operates at 125 kHz and locates the Rx position with no other communication module on the Rx. A real-time graphical interface displays the position of Rx. The system has a tracking frequency of 33 Hz, 1 cm^2 resolution and an average deviation of 6.8 mm.

References

[1] M. Schormans, et al., “Practical inductive link design for biomedical wireless power transfer: A tutorial,” in IEEE Trans. on Biomed. Circuits and Syst., vol. 12, no. 5, pp. 1112-1130, Oct. 2018.

[2] U. -M. Jow, et al., “EnerCage: A smart experimental arena with scalable architecture for behavioral experiments,” in IEEE Trans. on Biomed. Eng., vol. 61, no. 1, pp. 139-148, Jan. 2014.

[3] Y. Jia et al., “Position and orientation insensitive wireless power Transmission for EnerCage-Homecage System,” in IEEE Trans. on Biomed. Eng., vol. 64, no. 10, pp. 2439-2449, Oct. 2017.

[4] Z. Han, et al., “Moving receiver tracking in wireless power transfer systems,” 2022 29th IEEE Int. Conf. on Electron., Circuits and Syst. (ICECS), Glasgow, United Kingdom, 2022, pp. 1-4.

[5] J. Kim, et al., "Cage-Embedded crown-type dual coil wireless power transfer based microwave brain stimulation system for untethered and moving mice," in IEEE Trans. on Biomed. Circuits and Syst., vol. 17, no. 2, pp. 362-374, April 2023.

[6] M. Soma, et al., “Radio-Frequency coils in implantable devices: Misalignment analysis and design procedure,” in IEEE Trans. on Biomed. Eng., vol. BME-34, no. 4, pp. 276-282, April 1987.

[7] N. Soltani, et al., “Low-Radiation cellular inductive powering of rodent wireless brain interfaces: Methodology and design guide,” in IEEE Trans. on Biomed. Circuits and Syst., vol. 10, no. 4, pp. 920-932, Aug. 2016.

[8] D. Jiang, et al., “An integrated passive phase-shift keying modulator for biomedical implants with power telemetry over a single inductive link,” in IEEE Trans. on Biomed. Circuits and Syst., vol. 11, no. 1, pp. 64-77, Feb. 2017.

[9] W. Han, et al., "Accurate position detection in wireless power transfer using magnetoresistive sensors for implant applications," in IEEE Trans. on Magn., vol. 54, no. 11, pp. 1-5, Nov. 2018.